Interferometric measurements of stellar intensity profiles

Markus Wittkowski[a] and Christian A. Hummel[b]

[a]European Southern Observatory, Casilla 19001, Santiago 19, Chile

[b]U.S. Naval Observatory, 3450 Massachusetts Av. NW, Washington, DC 20392, USA

ABSTRACT

We report on direct interferometric measurements of stellar intensity profiles obtained with the Navy Prototype Optical Interferometer (NPOI) and the Very Large Telescope Interferometer (VLTI). These measurements need to make use of weak fringes, i.e. low visibility values, on resolved stars. We describe techniques that were used to obtain these low visibility values with high precision. They include the methods of baseline bootstrapping and wavelength bootstrapping, as well as, lately, coherent integration using phase bootstrapping. In addition, we developed methods to compensate photon and detection biases. We present recent measurements on the giant star γ Sge, obtained with the NPOI, which succeeded not only in discriminating between uniform disks and limb-darkened disks, but also in constraining Kurucz model atmosphere parameters. We present first VLTI measurements of visibility values beyond the first minimum which were taken on the giant star ψ Phe. Here, the capabilities to synthesize baselines of different lengths and to use different aperture sizes were used for the first time with the VLTI. We close with an outlook on the future potential on studies of stellar surface structure with the six-way beam combination at the NPOI and with the completed VLTI. This includes for instance direct measurements of the limb-darkened profiles of a large number of different types of stars, and of starspots which may for instance be caused by magnetic fields or large-scale photospheric convection.

Keywords: optical long-baseline interferometry, stellar atmospheres, stellar limb-darkening, stellar surface structure

1. INTRODUCTION

The precise measurements of the intensity profiles across stellar disks is of fundamental importance for our understanding of stellar atmospheres. These measurements are in principle only feasible to two or multi-aperture interferometers, since all stars except the sun and a very few apparently very large stars appear as point sources to current single-aperture telescopes. The comparison of measured stellar intensity profiles to model predictions allows us to test and constrain model atmospheres. This is an important complementary information in addition to observations of stellar spectra. As an example, Fig. 1 shows model predictions by the ATLAS model grid (14) for two stellar spectra (cool stars with low surface gravity), and for the corresponding derived limb-darkening parameters α ($I = \mu^{\alpha}$, with I the intensity and μ the cosine of the angle between the line of sight and the surface element of the star) for the wavelength range from 500 nm to 2200 nm. Owing to a lack of limb-darkening measurements, atmosphere models like these ATLAS models are usually only constrained by the stellar spectra, and not by spatially resolved observations of the limb-darkening effect. Fig. 1 illustrates that any single monochromatic or broad-band, i.e. filter averaged, limb-darkening measurement (determining directly the strength of the limb-darkening by measurements beyond the first minimum of the visibility function) can be used to be compared with models. Also, uniform-disk diameter variations with wavelength, which can even be derived by measurements before the first minimum of the visibility function, can be used. The most accurate and most promising approach is the comparison of spectrally resolved visibility measurements beyond the first minimum of the visibility function, without any intermediate approximation by a limb-darkening parameter. Such measurements can contribute significantly to new developments in stellar atmosphere modeling, as for instance to the development of new generation atmosphere models which are based on spherical symmetry instead of plane-parallelism. Furthermore, the exact intensity profiles can give important insights into more complicated atmospheres as for instance dynamical atmosphere models of pulsating stars which are influenced

E-mail: mwittkow@eso.org, cah@usno.navy.mil

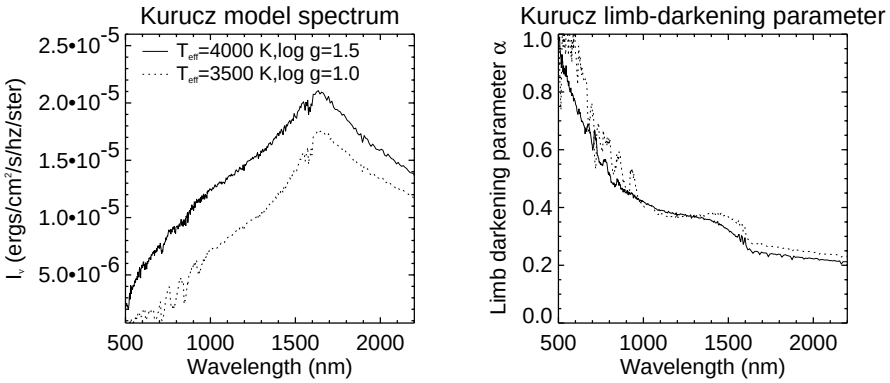

Figure 1. Examples of ATLAS model grid (Kurucz[14]) predictions for two stellar spectra and for the corresponding limb-darkening parameter.

by hydrodynamical effects as shocks. The final goal of these measurements is the reconstruction of images of stellar surfaces with several resolution elements across the stellar disk, revealing both the overall center-to-limb intensity variation and additional horizontal inhomogeneities as warm or cool starspots. These special surface features are expected to be caused by photospheric convection as well as by magnetic fields.

These required direct measurements of the intensity distributions of stellar disks are among the most challenging programs in modern optical interferometry. Since more than one resolution element across the stellar disk is needed to determine parameters beyond a diameter, the long baselines needed to obtain this resolution, i.e. to resolve the stellar disk, also produce very low visibility amplitudes. These low visibility amplitudes correspond to vanishing fringe contrasts. Hence, the corresponding fringes are difficult to be detected, tracked, and recorded. In addition, the data reduction of low visibility values is often a special challenge as well, since the contributions of photon noise and detection bias terms can be relatively high. Consequently, direct measurements of stellar surface structure parameters are rare. While diameters have so far been obtained by interferometric and lunar occultation methods for a large number of stars of the order of 1000, the second-order effect, limb-darkening, has been directly observed for only a very limited number of stars of the order of 10.

The NPOI (Navy Prototype Optical Interferometer), located at Lowell Observatory near Flagstaff, Arizona, is especially designed for imaging of stars and their environments and is described in detail by Armstrong et al.[1] . The methods of baseline bootstrapping and wavelength bootstrapping can be used in order to detect weak fringe contrasts. In January of 2002, the NPOI became the first optical interferometer to track and record stellar interference fringes with six telescopes simultaneously (2).

The ESO VLTI (Very Large Telescope Interferometer[5]), a European general user interferometer located on Cerro Paranal in northern Chile, is the largest astronomical instrument working at optical wavelengths in the world. It comprises four Unit Telescopes (UT, 8.2 m diameter), four movable Auxiliary Telescopes (AT, 1.8 m diameter), which can be positioned on thirty different stations, as well as a near-infrared beam-combination instrument (AMBER) and a mid-infrared beam-combination instrument (MIDI). The VLTI is currently in the phase of commissioning (17) with the near-infrared K-band commissioning instrument VINCI (13). In its completed phase, the VLTI will constitute an excellent facility for the imaging of stellar surfaces.

Here, we report on direct interferometric observations of the stellar limb-darkening effect by visibility measurements beyond the first minimum of the visibility function, obtained with the NPOI on the giant star γ Sge, and with VLTI and the VINCI instrument on the giant star ψ Phe. We concentrate on the description of the techniques that were used in order to obtain the low visibility amplitude values with high precision, and we present comparisons of our results with model atmospheres.

2. NPOI MEASUREMENTS OF THE GIANT STAR γ SAGITTAE

The interferometric observations of the giant star γ Sge were performed with the NPOI on July 21, 2000. A triangle of baselines with lengths of 18.9 m, 22.2 m, and 37.5 m was used and data were recorded in 32 spectral

channels ranging from 450 nm to 850 nm. This data set was first investigated by Wittkowski et al.[21] . Here, we report on the techniques that were used to track and record the low-contrast fringes on the long (37.5 m) baseline, and to reduce these low visibility data. In addition, we show the improvements by the more recent technique of coherent integration by phase bootstrapping (Hummel et al.[12]) on our data. Finally, we present the results that were obtained by a comparison of our direct multi-wavelength interferometric measurements of the limb-darkening effect with ATLAS model atmosphere predictions.

2.1. Observational techniques to obtain precise low visibility values

The observational techniques that were used to obtain precise visibility values despite the low fringe contrasts on the long (37.5 m) baseline include the use of baseline bootstrapping and wavelength bootstrapping, an accurate compensation of photon and detection biases, the use of triple products in addition to the squared visibility values, and, most recently, the coherent integration using phase bootstrapping.

Baseline bootstrapping and wavelength bootstrapping The NPOI is designed for the use as a bootstrapping array (see Armstrong et al.[1]). If, for an observation of a well-resolved star, a continuous chain of short baselines comprise a longer baseline, and if the higher-contrast fringes on the short baselines can be detected and tracked, the low-contrast fringes on the longer baseline are automatically stabilized, even if they could not be detected on the long baseline itself. For the example of our γ Sge NPOI measurements, the two shorter baselines with lengths 18.9 m and 22.2 m comprise the longer baseline with a length of 37.5 m. Given γ Sge's diameter and the effective spacings, the fringes on the shorter baselines corresponding to squared visibility amplitudes between 10% and 40% can well be detected and allow us to stabilize the weak-contrast fringes with squared visibility amplitudes of less than 1% on the long (37.5 m) baseline. In addition, with the use of a multi-wavelength beam-combiner and considering only one baseline, lower-contrast fringes in one spectral channel can be stabilized by using higher-contrast fringes in another spectral channel and hence another effective spacing (wavelength bootstrapping). Hajian et al.[7] demonstrated already that bootstrapping with the NPOI astrometric subarray enabled the measurement of visibility values of a resolved star beyond the first minimum of the visibility function.

Compensation of photon and detection biases For standard NPOI data reduction (see Hummel et al.[10]), the squared visibility amplitudes are derived by an incoherent average of raw data taken in 2 ms intervals. The real (X) and imaginary (Y) parts of the complex visibility are calculated for each baseline and spectral channel every 2 ms. The squared visibility amplitudes are calculated from these raw data using the unbiased estimator

$$|V|^2 = 4 \left[\frac{\pi/n}{\sin(\pi/n)}\right]^2 \frac{< X^2 + Y^2 - \sigma_I^2(N) >}{< N >^2}, \quad (1)$$

where $n = 8$ is the number of bins, N the total photon count rate in the coherent integration interval of 2 ms, and σ_I^2 the variance of the intensity caused by photon and detection noise. $|V|^2$ is compensated for background intensity by an additional factor $< N >^2 / < N - D >^2$, where D is the background rate. The use of a squared quantity requires attention to the bias σ_I^2. The noise bias term σ_I^2 is equal to N in case of Poisson statistics. Since the NPOI detectors exhibit non-Poisson noise, due to after-pulsing of the APDs, the noise bias is estimated by $\sigma_I^2 = Z^2$. Here, Z^2 is the fringe amplitude floor estimated at four times the modulation frequency (X and Y are calculated at the temporal frequency k=1 to select the component corresponding to the modulation frequency of the delay lines). This Z^2 compensation is often of sufficient accuracy for large visibility amplitudes. However, despite the Z^2 bias compensation, small positive visibility amplitudes are observed for fringe-less data and this bias, $B := |V|^2 \left(\text{fringe} - \text{less data}, \sigma_I^2 = Z^2,\ D = 0\right)$, was found to be a function of N and to be different for each spectral channel c and each spectrometer i. It was modeled with a power-law $B(i,c) = a_0(i,c)\, N^{a_1(i,c)}$ where parameters a_0 and a_1 were fitted to the fringe-less data. This additional bias was compensated by using $\sigma_I^2(N) = Z^2 + B\, N^2/f$ in Eq. 1. Fig. 2 illustrates the correctness of our bias compensation.

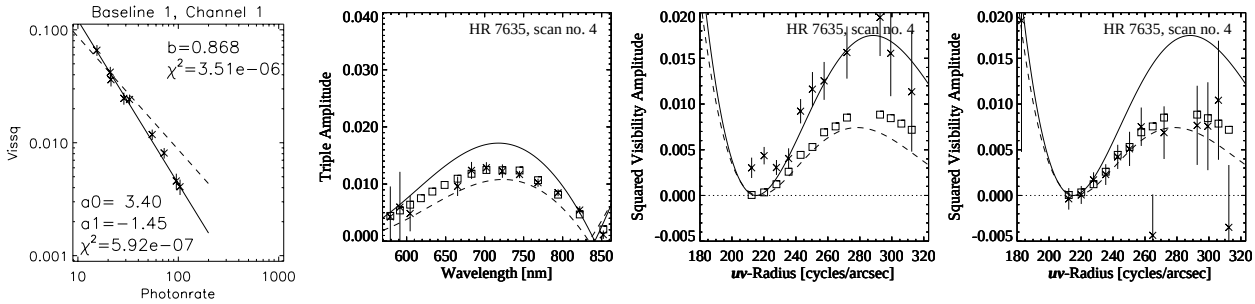

Figure 2. From left to right: (1) Squared visibility amplitudes as observed for fringe-less data after the Z^2 compensation (for one example), together with the fit of a power law as described in the text. (2) Triple amplitude values for this data which are free of any photon and detection bias terms. The observed values fit well a model prediction which is indicated by the squares. (3) Squared visibility values of the same data set after the Z^2 compensation, but before the additional B bias compensation. The observed values should follow the same model prediction as the unbiased triple amplitudes of the same data set. The B bias is evident in this plot. (4) Squared visibility of the same data set after the additional B bias compensation. The observed values follow the same model prediction as the unbiased triple amplitude values. This confirms the correctness of our bias compensation.

The use of triple amplitudes and closure phases The use of the triple product values, i.e. the triple amplitude and the closure phase, has several advantages as compared to the use of only the squared visibility amplitudes. The phase of the complex triple product formed by a triangle of baselines, i.e. the closure phase, is not corrupted by the phase noise caused by atmospheric turbulence. No bias correction is required for the triple product of our γ Sge NPOI data as described here, since the noise from the three detector arrays receiving the signal from each baseline is uncorrelated. In a triple with two short baselines and one long baseline resolving a stellar disk, as in the configuration used here, the triple amplitude has a higher signal-to-noise ratio than the squared visibility amplitude on the long baseline. This effect can be seen in our data. It can be understood due to the fact that the low visibility on the long baseline is not squared but multiplied with higher amplitudes from the other two baselines in the triple. This effect was also confirmed by simulations of visibility data based on Poisson noise. For the long baseline a visibility amplitude of 0.1 was assumed and for the two short baselines a visibility amplitude of 0.6. The signal-to-noise ratio of the squared visibility on the long (east-west) baseline was found to be 5 while that of the triple product was 20. In addition, predictions by different model atmospheres show usually stronger differences for the triple amplitudes than for the squared visibility amplitudes. Hence, models can more easily be constrained by the triple product measurements. Finally, the closure phase values are of essential importance for any detections of deviations from point symmetry of the object intensity distribution, i.e. for instance for the detection and imaging of starspots.

Coherent integration using phase bootstrapping The most recent development for NPOI data in order to obtain low visibility amplitudes on long baselines with high precision is the development of an algorithm to determine precise fringe phases in the presence of atmospheric turbulence. This allows us to employ a coherent integration of the complex visibility values over a longer range of time rather than the use of the incoherent average of the 2 ms data as described above. The recently obtained fringe phases are precise enough only for the larger signal-to-noise data obtained on the two shorter baselines. However, the use of these fringe phases together with the closure phase enables the determination of the lower signal-to-noise fringe phase on the longer baseline (phase bootstrapping). This algorithms is described in detail by Hummel et al.[12] . In a sense, it implements a phase tracking interferometer in the offline data reduction. The coherent average of the complex visibility values results in a higher signal-to-noise ratio of all our γ Sge data, the squared visibility values, the triple amplitudes, and the closure phases. Furthermore, the additional bias B is described above is significantly lower since it was found to be about inversely proportional to the photon count rate during the coherent integration time (see above).

2.2. Results and comparison to models

Fig. 3 shows our resulting NPOI γ Sge squared visibility amplitudes (left), triple amplitudes (middle), and closure phases (right) for the example of one out of a total of six obtained scans. The upper row shows the

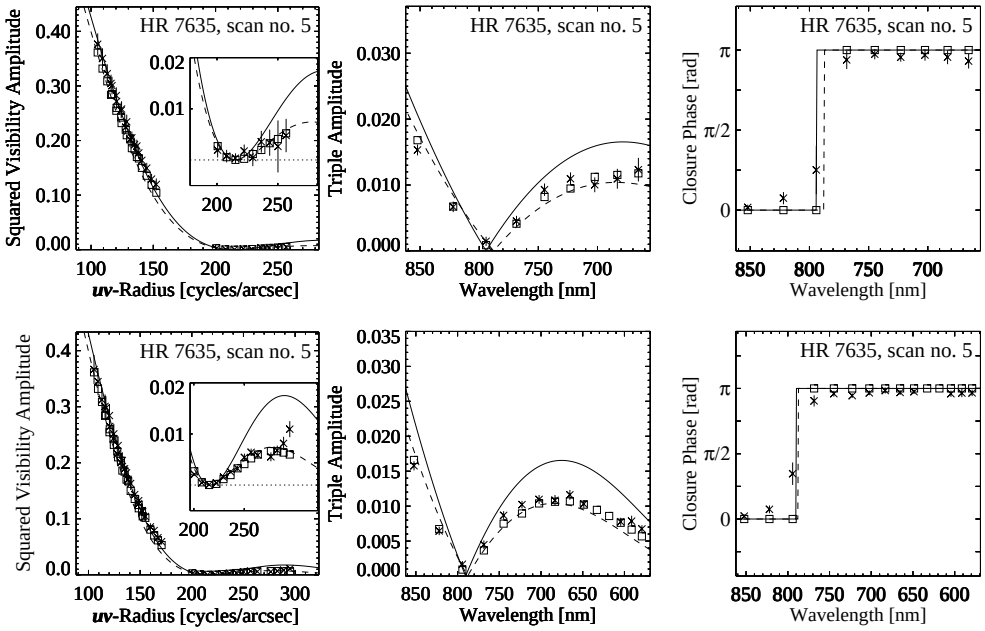

Figure 3. Squared visibility amplitudes (left), triple amplitudes (middle), and closure phases (right) of one scan of our NPOI γ Sge data. The upper row shows the values obtained by the incoherent average as shown in Wittkowski et al. (2001). The lower row shows the results obtained with the most recent algorithm using a coherent integration using phase bootstrapping (Hummel et al., these proceedings). The values obtained with the coherent integration show, as expected, lower error bars, and a larger number of spectral channels can be employed.

results obtained with the incoherent average of the squared visibility amplitude and triple product values as shown in Wittkowski et al.[21] . Due to the lower signal-to-noise of the blue NPOI channels, only the 10 reddest spectral channels were used for this analysis. The lower row shows the results obtained with our most recent method, the coherent integration of the complex visibility values. This new algorithm results in smaller error bars, and, as a result, allows us also to use a lager number of spectral channels. Hence, it can be expected that comparisons with models can now be performed with higher significance than before.

Based on the data obtained by the incoherent average, the following reduced χ^2_ν values were obtained by fitting all our measured γ Sge visibility data to model atmosphere predictions on a grid of assumed effective temperatures and surface gravities.

$\log g$/ $T_{\rm eff}$ [K]	0.0	0.5	1.0	1.5	2.0	2.5
3500	1.50	1.40	1.35	1.38	1.47	1.58
3750	1.29	1.29	1.29	1.29	1.27	1.26
4000	1.18	1.17	**1.17**	1.17	1.18	1.18
4250	1.20	1.20	1.19	1.19	1.19	1.19
4500	1.26	1.25	1.24	1.23	1.23	1.23

The χ^2_ν values show a well defined minimum at $T_{\rm eff}$=4000 K and $\log g$[cgs]=1.0. The values around this minimum as functions of $\log g$ and $T_{\rm eff}$ follow a well defined parabola, as expected near the minimum of the χ^2_ν function. The analysis of the parabola results in most likely values of $T_{\rm eff} = 4160 \pm 90$ K and $\log g = 0.9 \pm 1.0$. These values are in good agreement with independent estimates. The minimum χ^2_ν value of 1.17 is close to the optimum

value of 1.0 and shows that the ATLAS model prediction (14) fits our measured data well, and in particular considerably better than uniform disk ($\chi^2_\nu = 4.36$) and fully-darkened disk ($\chi^2_\nu = 2.26$) models. It is expected that model predictions can be tested with even higher significance using the higher precision visibility values obtained with our new algorithm of coherent integration as described above. Our data will also be able to give important constraints for the development of new generations of model atmospheres. For instance, it is expected that newly developed PHOENIX[9] and MARCS[6] atmosphere models for giant stars based on spherical symmetry rather than on plane parallelism describe observed visibility data of giant stars considerably better.

3. VLTI MEASUREMENTS OF THE GIANT STAR ψ PHOENICIS

VLTI measurements of visibility amplitudes beyond the first minimum of the visibility function succeeded already during the VLTI commissioning phase on the resolved giant star ψ Phoenicis using the near-infrared K-band two-beam commissioning instrument VINCI. Here, the capability to synthesize baselines of different lengths and with different aperture sizes was used for the first time with the VLTI. High visibility values obtained in October 2001 on a 16 m baseline using the VLTI test siderostats were combined with low visibility values beyond the first minimum of the visibility function obtained on November 1 and 2, 2001 on a 102 m baseline using the 8.2 m diameter VLTI Unit Telescopes.

3.1. Observational techniques to obtain precise low visibility values with VLTI/VINCI

The VLT interferometer will provide bootstrapping configurations with the AMBER instrument, a near-infrared instrument which can combine three beams simultaneously, similar to the bootstrapping configurations of NPOI as described above. Furthermore, with the fringe tracker FINITO, VLTI will constitute a real-time phase-tracking interferometer. However, these functionalities are not yet available during the commissioning phase with the VINCI instrument. The observational techniques to obtain low visibility amplitude values beyond the first minimum of the visibility function with high precision include for the time being the use of single-mode optical fibers and the use of apertures of different sizes for different baseline lengths.

The use of different aperture sizes for different baselines lengths For our VLTI/VINCI ψ Phe measurements, the VLTI test siderostats with an aperture diameter of 40 cm were used with the 16 m baseline. The expected relatively high squared visibility amplitude of about 80% for this baseline can well be measured with this aperture size. For the required measurements of the very low squared visibility amplitudes of only about 1% beyond the first minimum of the visibility function, however, the for this needed 102 m baseline was used with the giant 8.2 m diameter UT telescopes. As a result, the signal-to-noise ratio of these extremely low-contrast fringes is of similar order as that of the high-contrast fringes on the short baseline with the siderostats. The layout of this VLTI configuration is illustrated in Fig. 4. The exploited effect can also be understood by looking at the correlated magnitudes with respect to the limiting magnitudes of the different telescope apertures:

Telescope	Baseline (m)	Lim. magn.	V^2	K magn.	Corr. K magn.	Difference to lim. magn.
Sid.	16	~ 1	0.8	-0.63	-0.39	1.4
UT	102	~ 6	0.01	-0.63	4.37	1.6

At the time of these observations, the VLTI siderostats had a limiting K magnitude of about 1, while the limiting K magnitude of the UTs was about 5. The UTs were not equipped with an adaptive optics system, so the effectively used aperture was smaller than full 8.2 m diameter aperture. The ψ Phe diameter of about 7.8 mas leads to squared visibility values on the 16 m and 102 m baselines of about 0.8 and 0.01, respectively. With the ψ Phe K magnitude of -0.63, the correlated K magnitudes for the two baselines are -0.39 and 4.37, respectively. Both values are by about 1.5 mag below the respective limiting magnitudes of the siderostats and the UTs.

Configurations using different aperture sizes for different baseline lengths as the one used here are an interesting perspective for the completed VLTI as well. For imaging campaigns of stars, it will be mandatory to obtain visibility data evenly distributed over the *uv*-plane including high-contrast fringes as well as very

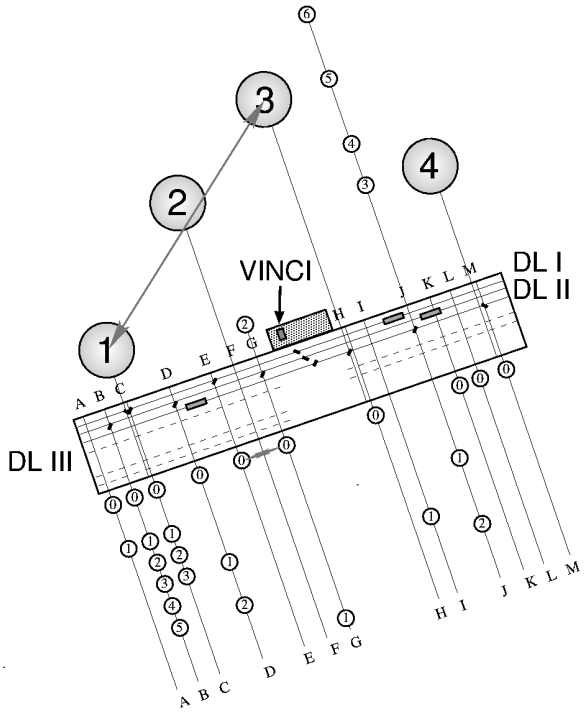

Figure 4. General layout of the VLTI. Shown are the positions of the 4 UTs, the 30 AT stations, the system of light ducts, the delay line tunnel with the currently existing three delay lines, and the interferometric lab with the commissioning instrument VINCI. The configuration used for our ψ Phe measurements is indicated by the arrows. The 16 m E 0-G 0 baseline with the 40 cm test siderostats was combined with the 102 m UT 1-UT 3 baseline with the 8.2 m diameter UT telescopes (an effective aperture of smaller diameter was used since these telescopes were not yet equipped with adaptive optics). This configuration ensures that the extremely low-contrast fringes on the long 102 m baseline show a similar signal-to-noise ratio as the high-contrast fringes on the short baseline.

low contrast fringes in the second, third, and following lobes of the visibility function. Then, the lowest fringe contrasts can be measured with the UTs in order to obtain a sufficient signal-to-noise ratio while higher fringe contrasts on the same target can be obtained with the ATs.

The use of single-mode optical fibers The VINCI instrument spatially filters the two incoming beams by single-mode fibers before they are combined. Hereby, the single-mode fibers transform phase distortions into intensity fluctuations. These fluctuations can easily be monitored, and the interferograms can be corrected from the photometric fluctuations. This technique is generally known to lead to very accurate object visibility measurements (3).

3.2. Observations and data reduction

The general layout of the VLTI system is shown in Fig. 4. The two afocal beams of light from either the two siderostats or the two UTs are reduced in diameter and sent through an underground light duct system to the interferometric tunnel where they are compensated for optical path differences by delay-lines. The beams are then directed into the interferometric laboratory, again reduced in diameter and sent to the VINCI instrument where they are focused onto single-mode optical fibers and afterwords combined by a fiber beam combiner providing two interferometric outputs. Before beam combination, the photometric signals are separated from each of the two input beams in order to monitor the photometric fluctuations. The two interferometric and two photometric output signals are imaged through a K-band filter onto a near-infrared Hawaii array where

they are detected. The fringes are detected by modulation of the optical path difference with an amplitude of typically 200 μm to 300 μm using a piezo element within the VINCI instrument, and kept within the scan length by sending an offset signal to the delay lines after every scan of about 0.5 sec.

VLTI/VINCI data on ψ Phe on the 16 m baseline using the siderostats were recorded during 6 nights in October and November 2001. The fringe frequency was 287 Hz. Most of these nights show strong variations of the atmospheric seeing and coherence time resulting in unstable atmospheric transfer functions over the night. For the analysis presented here, only the night starting on October 17 was used when the transfer function was measured to be most stable. Work is in progress to develop methods to better calibrate data taken during unstable nights. Data on the 102 m baseline using the VLT Unit Telescopes were recorded during the nights starting on November 1 and 2, 2001, with a fringe frequency of 677 Hz. During all nights, several series of interferograms were obtained on ψ Phe and several calibrators. The calibrators for the 16 m baselines have, owing to the limiting magnitude, diameters between 3 mas and 6 mas. In this range, special attention has to be paid on the adopted diameter values. All calibrator diameters were adopted by taking an average over different estimates and measurements. A VLTI calibrator program in order to derive calibrator diameters in a self-consistent way is in progress (Percheron et al.[15]). The squared coherence factors were obtained for each interferogram using an algorithm following the method described by Foresto et al.[3] . The resulting coherence factors μ_1^2 and μ_2^2 for each of two interferometric outputs were edited and averaged over a series (batch) of 300 to 500 interferograms. For the calibrator stars, the transfer functions t_1^2 and t_2^2 were computed as $t_i^2 = \mu_i^2/V^2$ where V^2 is the predicted visibility using the adopted diameter values. The transfer function values for the time of any of the ψ Phe observations were obtained as a weighted average of the observed t_i^2 values with the weight being a product of (1) a Gaussian function of the time difference from the target measurement with a σ of 1 hour, and (2) the error of the single transfer function measurement (consisting of the statistical error and the error resulting from the limited accuracy of the adopted diameter value). The final ψ Phe squared visibility values are then obtained by dividing the ψ Phe coherence factors by the transfer function values obtained for the respective time, and averaging of the two values from the two interferometric outputs.

As mentioned above for the NPOI data reduction, the knowledge of possible remaining biases for fringe-less data, i.e. data for which the correct visibility values are known to be zero, is essential for an analysis of very low fringe contrasts. Fringe-less data on several stars of different magnitudes were taken with VLTI/ VINCI in May 2002 by moving the delay lines off the fringe-packet. Only the siderostats were used for these measurements. There is a high probability to obtain considerable biases for fringe-less data in the very low signal-to-noise regime which decreases very rapidly with increasing photometric signal-to-noise ratios. For standard observations with the siderostats, biases for the coherence factors of up to 1% - 2% have to be expected. Work is in progress in order to better understand the origin of these bias terms and to compensate them. The effect of these terms is low for high visibility values. For the low fringe contrasts measured for ψ Phe, these terms are expected to be negligible since the photometric signal-to-noise ratios obtained with the UTs are by a factor of about 100 larger than for these data obtained with the siderostats. It is planned to record fringe-less data with the UTs as well, in order to test the data and the data reduction for possible remaining biases in this high photometric signal-to-noise regime.

3.3. Results and comparison with models

Fig. 5 shows the resulting squared visibility amplitudes for the VLTI/VINCI ψ Phe data. This figure shows that precise measurements of squared visibility amplitudes beyond the first minimum of the visibility function can be obtained with the VLTI in the configuration as described above and employing the commissioning instrument VINCI. The best fitting models of a uniform disk, a fully darkened disk, and a ATLAS model atmosphere for a M4 giant star result in the following values for the ψ Phe diameter Θ and the reduced χ_ν^2 values:

Model	Θ	χ_ν^2
UD	7.39 mas	1.0
FDD	8.74 mas	1.8
ATLAS model	7.75 mas	0.3

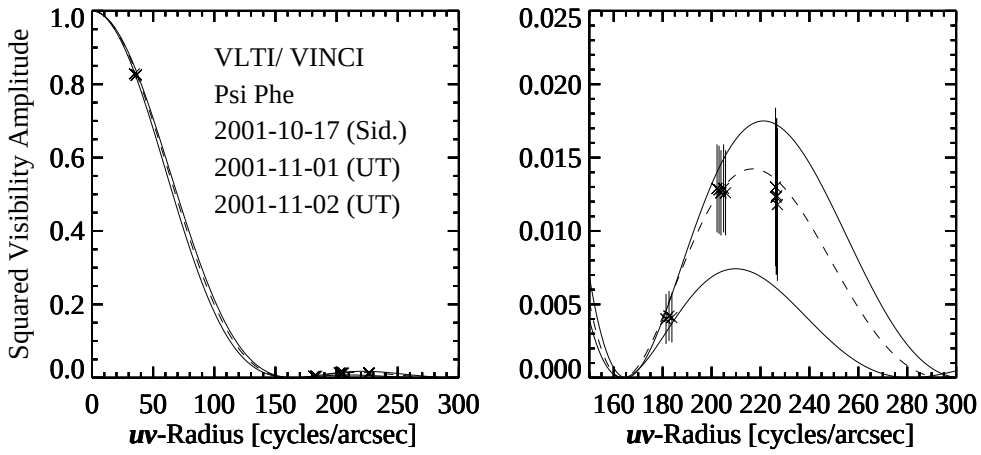

Figure 5. Squared visibility amplitudes of ψ Phe together with best fitting models of a uniform disk (upper solid line), of a fully darkened disk (lower solid line), and of a ATLAS model atmosphere for this object (dashed line). The right panel shows an enlarged view of the low values in the left panel.

The diameter error for each of these model assumptions is estimated to be $\sim$3%. As expected, the ATLAS model atmosphere is a considerably better model than the uniform disk and fully darkened disk models. The low χ^2_ν value of 0.3 indicates that the error bars for the squared visibility amplitudes as shown in Fig. 5 are over-estimated and can likely be reduced by about a factor of 2. The derived limb-darkened ψ Phe diameter is in good agreement with an estimate obtained with an empirical correlation by Dyck et al.[4] which results in a value of 8.0 mas $\pm$ 0.4 mas. It is also remarkable that the uniform disk model is a better model than the fully darkened disk model. This is expected by model atmospheres, as shown in Fig. 1. The limb-darkening models for stars similar to ψ Phe show a transition from being close to a fully darkened disk model ($\alpha = 1$) at wavelengths around 500 nm to being closer to a uniform disk model ($\alpha = 0$) at wavelengths around 2 μm. Consistently, the NPOI data of γ Sge at optical wavelengths, on the contrary, can better be described by a fully-darkened disk model than by a uniform disk model.

4. SUMMARY AND OUTLOOK

The NPOI measurements of the giant star γ Sagittae as well as the VLTI/ VINCI measurements of the giant star ψ Phoenicis confirm both that optical interferometry is now able to obtain information on intensity profiles across individual stellar disks beyond diameter measurements. This becomes possible by the use of several techniques in order to obtain low fringe visibility values with high precision, including bootstrapping techniques, the use of triple products, accurate compensations of detection and photon noise bias terms, coherent fringe integration, the use of single-mode optical fibers, and the use of different aperture sizes for different baseline lengths. The derived information on the stellar intensity profiles is important for our understanding of stellar atmospheres and, hence, of stellar structure and evolution. Our comparisons with models show that these measurements can be used to test and constrain models for stellar atmospheres. These spatially and spectrally resolved measurements will provide important observational constraints for tests tests of current and the developments of next generation model atmospheres as for example MARCS[6] and PHOENIX[9] models which take spherical symmetry into account. With the rapidly evolving technology of interferometry, future measurements employing for instance the simultaneous combination of 6 beams at the NPOI with baselines of up to 437 m, or employing the VLTI with its 1.8 m Auxiliary Telescopes and 8.2 m Unit Telescopes and baselines of up to 200 m, will very soon be able to derive even more precise information on stellar intensity profiles of a wide range of stars. One of the goals is for example to obtain consistent spectrally resolved measurements of the limb-darkened profiles of stars with compact atmospheres across the Hertzsprung-Russel diagram as an input for current and future atmosphere modeling. Further applications are for instance the comparison of measurements of extended atmospheres and winds of pulsating stars with dynamical model atmospheres. Fig. 6 shows as an example the high-precision VLTI/ VINCI visibility function of the prototype Mira star o Cet (see also Richichi et al.[16]),

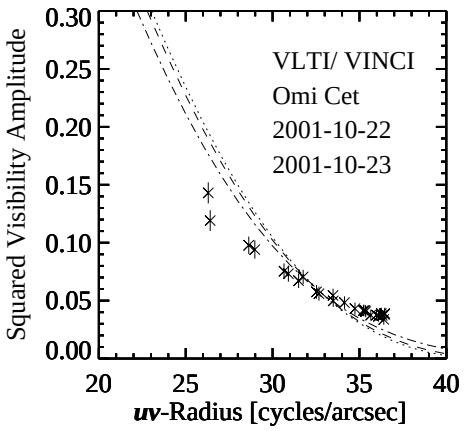

Figure 6. VLTI/ VINCI visibility curve of the prototype Mira star o Cet based on data obtained in the nights starting on October 22 and 23, 2001 (see also Richichi et al.[16] and in preparation). Any single symmetric one-component model for the intensity distribution I of the form $I = \mu^\alpha$ can not fit the data. Shown are best fitting models of a uniform disk ($\alpha = 0$, dotted line), of a fully darkened disk ($\alpha = 1$, dashed line) and a Gaussian-like disk ($\alpha = 5$, dashed-dotted line).

which can not be described by a single symmetric one-component intensity profile I of the form $I = \mu^\alpha$ with any parameter α, a form which was found to be able to describe well a wide range of static model atmospheres.

The final goal of these measurements is the reconstruction of images of stellar surfaces with several resolution elements across the stellar disk, revealing both the overall center-to-limb intensity variation, i.e. the vertical temperature structure, and additional horizontal temperature inhomogeneities as warm or cool starspots. These surface features are expected to be caused by photospheric convection as well as by magnetic fields. The feasibility to derive information on starspots was investigated and confirmed for the completed NPOI by Hummel[11] and Wittkowski,[20] and for the completed VLTI by von der Lühe et al.,[18] Hatzes,[8] von der Lühe,[19] and Wittkowski et al.[22] .

ACKNOWLEDGMENTS

The VLTI and NPOI measurements were made possible by the whole VLTI group at ESO and the whole NPOI group, respectively. The NPOI group is a cooperation of scientists at the US Naval Observatory, the Naval Research Laboratory, and the Lowell Observatory. The NPOI is funded by the Office of Naval Research and the Oceanographer of the Navy. The VLTI results on ψ Phe and o Cet are based on public data released from the VLTI. MW is grateful to Pascal Ballester, Pierre Kervella, Cyrus Sabet, Markus Schöller, and Rainer Wilhelm for providing the data reduction software for VLTI/VINCI scan data. MW acknowledges major contributions by Bill Cotton to the development of IDL tools to edit, average, and calibrate the single scan VLTI/VINCI values.

REFERENCES

1. J. T. Armstrong, D. Mozurkewich, L.J. Rickard, D.J. Hutter, J.A. Benson, P.F. Bowers, N.M. Elias II, C.A. Hummel, K.J. Johnston, D.F. Buscher, J.H. Clark III, L. Ha, L.-C. Ling, N.M. White, and R.S. Simon, "The Navy Prototype Optical Interferometer", *Astrophys. J.* **496**, pp. 550-571, 1998
2. J.A. Benson, C.A. Hummel, D. Mozurkewich, "Simultaneous 6-station observations with the NPOI", in *Proc. SPIE* **4838**, W. A. Traub ed., 2002 (these proceedings)
3. V.C. de Foresto, S. Ridgway, J.-M. Mariotti, "Deriving object visibilities from interferograms obtained with a fiber stellar interferometer", *Astron. Astrophys. Suppl. Ser.* **121**, pp. 379-392, 1997
4. H.M. Dyck, G.T. van Belle, S.T. Ridgway, "Radii and Effective Temperatures for K and M Giants and Supergiants", *Astron. J.* **111**, 1705-1712
5. A. Glindemann et al., "Very large telescope interferometer: a status report", in *Proc. SPIE* **4838**, W. A. Traub ed., 2002 (these proceedings)
6. B. Gustafsson, B. Edvardsson, K. Eriksson, M. Mizuno-Wiedner, B. Plez, "A Grid of Model Atmospheres for Cool Stars", *Proc. IAU Symp. 210*, in press, 2002
7. A.R. Hajian, J.T. Armstrong, C.A. Hummel, et al., "Direct Confirmation of Stellar Limb Darkening with the Navy Prototype Optical Interferometer", *Astrophys. J.* **496**, pp.484-489

8. A.P. Hatzes, "Indirect Imaging of Stellar Surface Structure", in *Science with the VLT Interferometer*, F. Paresce (ed.), pp. 293-302, 1997
9. P.H. Hauschildt, F. Allard, J. Ferguson, E. Baron, D.R. Alexander, "The NEXTGEN Model Atmosphere Grid. II Spherically Symmetric Model Atmospheres for Giant Stars with Effective Temperatures between 3000 and 6800 K", *Astrophys. J.* **525**, pp. 871-880 ,1999
10. C.A. Hummel, D. Mozurkewich, J.T. Armstrong, A.R. Hajian, N.M. Elias II, D.J. Hutter, "Navy Prototype Optical Interferometer Observations of the Double Stars Mizar A and Matar", *Astron. J.* **116**, pp. 2536-2548, 1998
11. C.A. Hummel, "Imaging and Modeling of Binaries with NPOI", in *ASP Conf. Ser.* **194**, S.C. Unwin and R.V. Stachnick eds., pp. 44-50, 1999
12. C.A. Hummel, D. Mozurkewich, J.A. Benson, M. Wittkowski, "Coherent integration using phase bootstrapping", in *Proc. SPIE* **4838**, W. A. Traub ed., 2002 (these proceedings)
13. P. Kervella, et al., "VINCI, the VLTI commissioning instrument: status after one year of operations", in *Proc. SPIE* **4838**, W. A. Traub ed., 2002 (these proceedings)
14. R. Kurucz, "Limbdarkening for 2 km/s grid", Kurucz CD-ROMs, Cambridge, Mass.: Smithsonian Astrophysical Observatory, 1993
15. I. Percheron, A. Richichi, M. Wittkowski, "Getting ready for high accuracy measurements: The VLTI Calibrators Program", in *Proc. SPIE* **4838**, W. A. Traub ed., 2002 (these proceedings)
16. A. Richichi, M. Wittkowski, M. Schöller, "High-precision measurements of cool giant stars with the ESO VLT Interferometer", in *Mass-losing Pulsating Stars and their Circumstellar Matter*, Y. Nakada and M. Honma (eds.), 2002, in press
17. M. Schöller, et al., "Commissioning the VLT interferometer: from first fringes towards a general user facility", in *Proc. SPIE* **4838**, W. A. Traub ed., 2002 (these proceedings)
18. O. von der Lühe, S. Solanki, T. Reinheimer, "Observing stellar surface structure with the ESO-VLT interferometer", in *Proc. IAU Symp. 176, Stellar Surface Structure*, Strassmeier and Linsky (eds.), pp. 147ff, 1996
19. O. von der Lühe, "Stellar Surface Observations with the VLTI", in *Science with the VLT Interferometer*, F. Paresce (ed.), pp. 303-315, 1997
20. Wittkowski, M.,"Computer simulations of interferometric studies of stellar surface structures with NPOI", *BAAS* **32**, 684, 2000
21. M. Wittkowski, C.A. Hummel, K.J. Johnston, D. Mozurkewich, A.R. Hajian, N.M. White, "Direct multiwavelength limb-darkening measurements of three late-type giants with the Navy Prototype Optical Interferometer", *Astronomy & Astrophys.* **377**, pp. 981-993, 2001
22. M. Wittkowski, M. Schöller, S. Hubrig, B. Posselt, O. von der Lühe, "Measuring starspots on magnetically active stars with the VLTI", *Astron. Nachr./ AN* **323**, pp. 241-250, 2002